# Systemic Logic in Theoretical Astrophysics

**Igor Makarov**

**Reform Science Center (*info@reformscience.org*)**

This is the presentation of my 30-year-long independent research in Systems Theory and Theoretical Physics. **Results:**
(1) **the research initiates the reform of modern physics,**
**(2) gives the true interpretation of the Systems Theory,**
**(3) paves the way to the reform of science in general.**

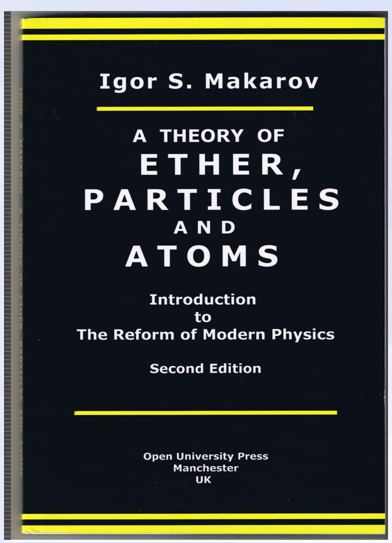


Its four parts were published in the Indian Journal of Theoretical Physics (1996-2005). In 2007 it was printed privately as a book ***"A Theory of Ether, Particles and Atoms"***, its copies sent to some Western academies.

Its second edition is now available in print and online, http://kvisit.com/S2uuZAQ.

# 2. Features of the method

The research is based on Hegel's dialectical logic**.** The method is called ***'the method of systemic intuition'***. Every step a discovery. We discover first the **ORIGIN** of the object, reveal its **ESSENCE**, develop its **PROJECT** and then realize it into **TRUE THEORY.**

According to the philosophy underlying this method, **truth cannot be observed, it can only be thought;** so the results obtained with this method cannot be confirmed directly by experiment. At the same time this method takes into account all achievements of modern science and can explain any experimental fact.

**THIS METHOD SOLVES PROBLEMS BEYOND THE REACH OF MODERN SCIENCE.**

# 3. The main results

**(1)** only two fundamental particles – virtual electron and positron; their interaction leads to virtual positronium generating energy;
**(2)** ether consists of virtual positroniums exchanging photons;
**(3)** in ether there takes place spontaneous generation of mesons and neutrons; cosmic rays and CMB are proper radiations of ether;
**(4)** the essence of nuclear interaction is conservation of energy by alternate transformation of electric energy to magnetic one and vice versa, the D-atom (deuterium) being its fundamental case;
**(5)** seven nuclear shells of 2, 8, 18, 36, 18, 8 and 2 D-atoms;
**(6)** all atoms can be modeled by electric LCR-networks;
**(7)** excited by photons, atoms responds with neutrinos;
**(8)** the structure of the $^{238}$U-atom reveals the implicit structure of the H-atom; it is the most perfect model of ether;
**(9)** radius of the electron is ~ 0.01 fm - instead of modern 2.82 fm.

# 4. Theory of ether

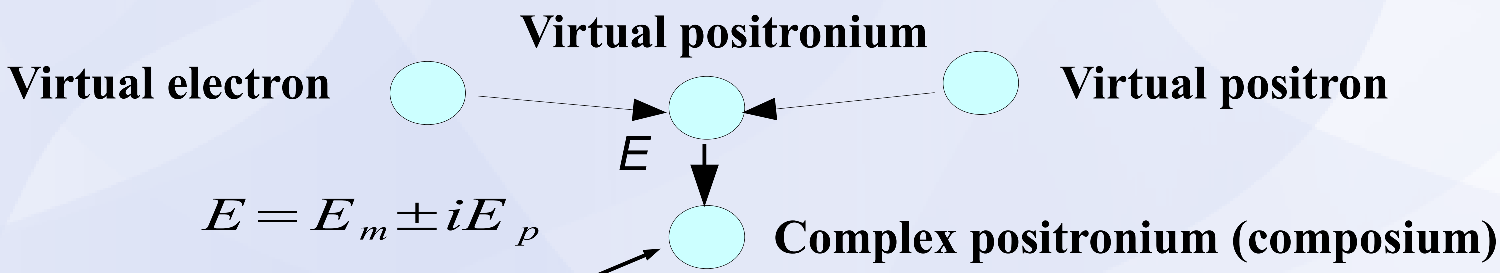


$$E = E_m \pm iE_p$$

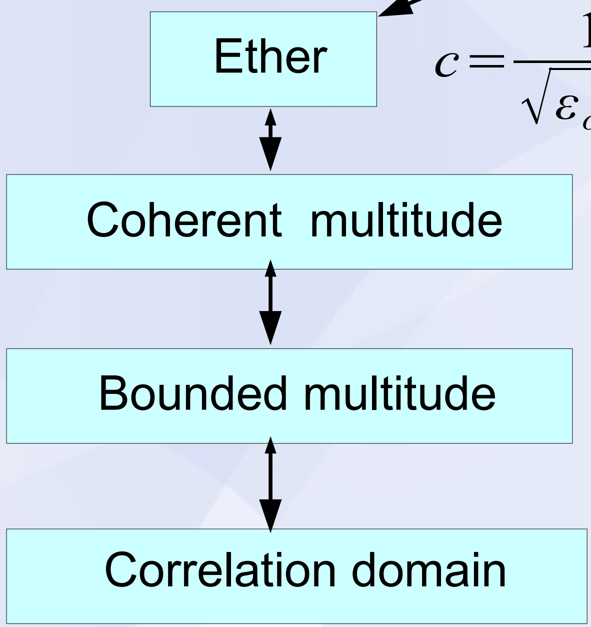


$$c = \frac{1}{\sqrt{\varepsilon_o \mu_o}}$$

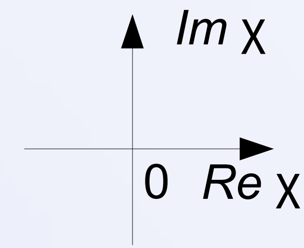


$$\chi = \frac{2\pi E}{hc}; \quad \Re\chi < 0$$

$$\varphi_\chi(s) = \mathrm{e}^{\chi s}; \quad s = r = ct$$

$$C_\chi = A_\chi \pm iB_\chi$$

**Complex spectrum of ether**

$$S(\chi) = \frac{dC_\chi}{d\chi}$$

**Correlation function of ether**

$$g(s) = \frac{1}{2\pi i}\int_L S(\chi)\,\mathrm{e}^{\chi s}\,d\chi; \quad \Re\chi \geq 0$$

# 4. Cosmic rays and ether

Experiments suggest the following spectrum of cosmic rays photons:

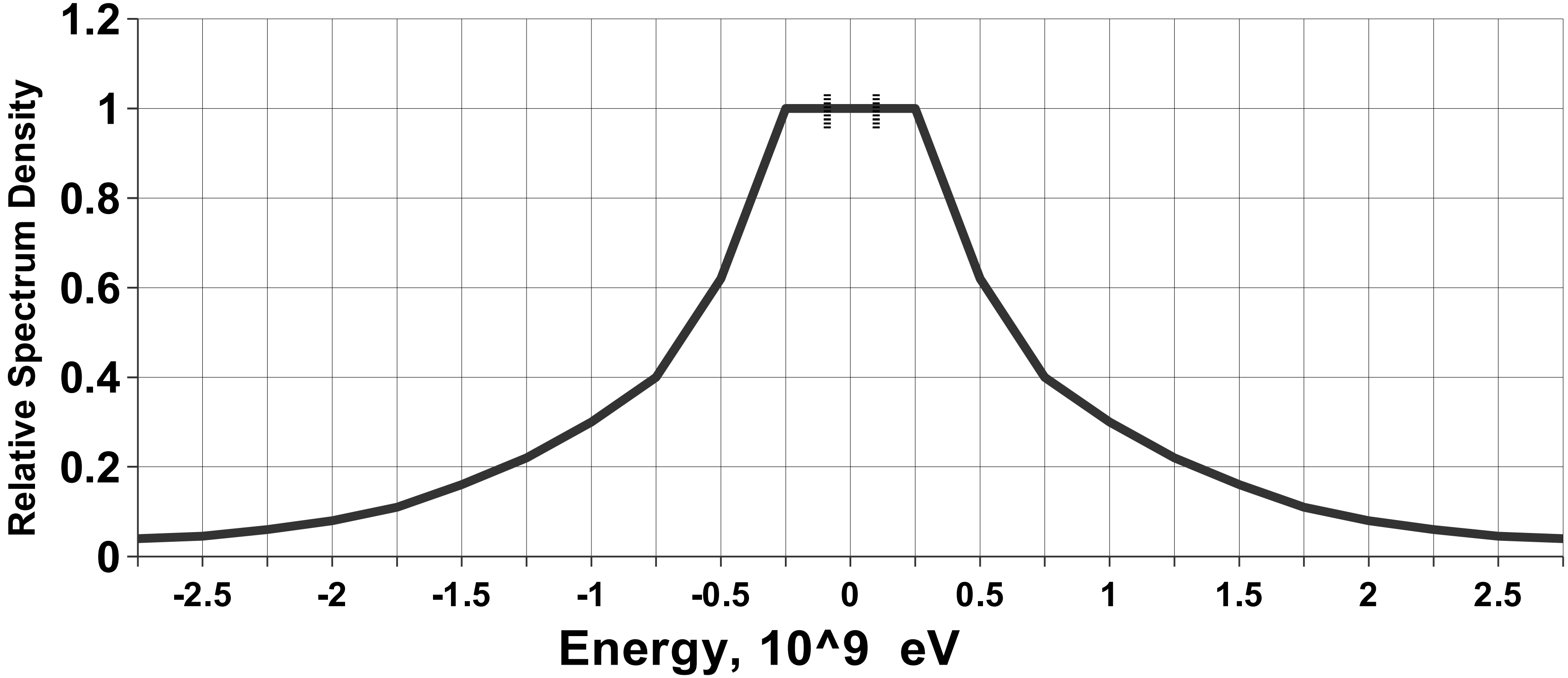


Spectrum of cosmic rays photons

# 6. Formulas for computation

The piece-wise approximation of the spectrum of ether:

$$\log P(E_{eV}) = \begin{cases} 0; & 0 \le \log E \le 8.5 \\ 8.5 - \log E; & 8.5 \le \log E \le 9.0 \\ 15.7 - 1.8 \log E; & 9.0 \le \log E \le 9.5 \\ 24.06 - 2.68 \log E; & 9.5 \le \log E \end{cases}$$

The first power of the spectrum on a linear scale:

$$SPHE(E) = 10^{\mathbf{0.5 \log P(E)}}$$

The correlation function of ether

$$g(r) = \frac{1}{2\pi i} \int_L S(z) e^{zr} dz; \quad z = x + iy; \quad x \ge 0$$

The complex spectrum of ether

$$S(z) = F(x, y) e^{i\varphi(x, y)}$$

$$\ln S(z) = \ln F(x, y) + i\varphi(x, y); \quad f(x, y) = \ln F(x, y)$$

Poisson's formula

$$f(x_0, y_0) = \frac{x_0}{\pi} \int_{-\infty}^{\infty} \frac{f(0, y) dy}{(y - y_0)^2 + x_0^2};$$

Cauchy-Riemann conditions

$$\frac{\partial f}{\partial x} = \frac{\partial \varphi}{\partial y}, \quad \frac{\partial f}{\partial y} = -\frac{\partial \varphi}{\partial x};$$

Argument of the spectrum

$$\varphi(x, y) = \int_{y_1=0}^{y} \frac{\partial f(x, y_1)}{\partial x} dy_1;$$

$$f(0, y) = \ln SPHE(y); \quad SPHE(0) > 0$$

# 7. Correlation function of ether

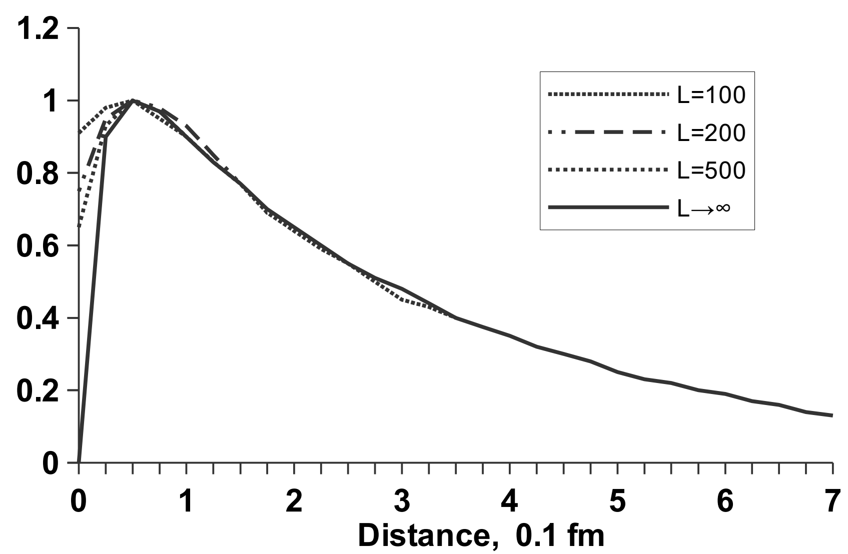


**Correlation function of ether**

The computation was performed in three ranges of energy, $1.26\times10^{10}\,eV$, $2.52\times10^{10}\,eV$, $6.3\times10^{10}\,eV$, corresponding to parameters L=100, L=200 and L=500, respectively. The bold line corresponds to approximation (L= $\infty$).

# 8. Correlation function. Detail

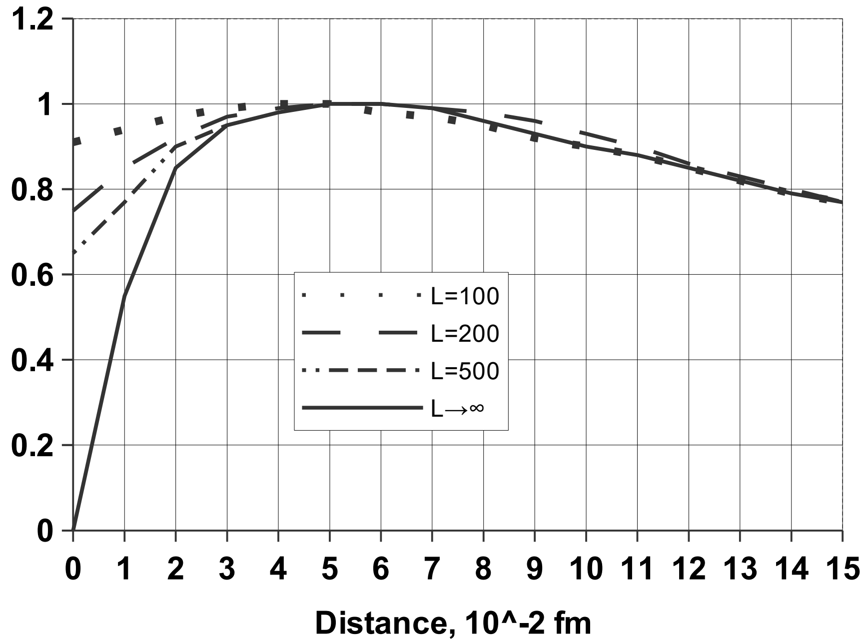


Correlation function of ether. Detail

# 9. Characteristics of ether and particles

The correlation function (high energy region): $g(r) \propto \exp(-\alpha_{et} r) - \exp(-\beta_{et} r)$

Its radius of extrema: $r_{et} \approx 5.2 \times 10^{-2}\ fm$

The spectrum of ether in high energy region: $|S(i\omega)|^2 \propto \dfrac{1}{(\alpha_{et}^2 c^2 + \omega^2)(\beta_{et}^2 c^2 + \omega^2)}$

The rate of photon exchange: $\alpha_{et} = 3.18\ fm^{-1}$

The rate of corpuscular interaction: $\beta_{et} = 56.81\ fm^{-1}$

Singularity distribution function: $\varphi_o(q) = \dfrac{2\beta_{et}^3}{\pi^2} \exp(-2\beta_{et}|q|);\quad \sqrt{\overline{q^2}} = 1.24 \times 10^{-2}\ fm$

## Dimensions of particles

Electron: $r_e \approx 0.01\ fm$ (in modern theory: $r_e \approx 2.82\ fm$ )

Muon: $r_m \approx 0.19\ fm$

Neutron: $r_n \approx 0.46\ fm$ , which corresponds to modern experimental data, 0.3 *fm* to 0.5 *fm*.

# 10. Spontaneous generation of particles

## Muon

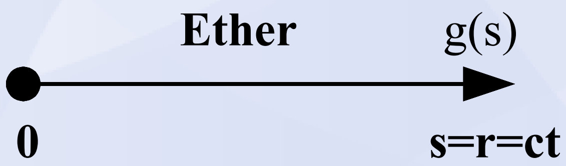


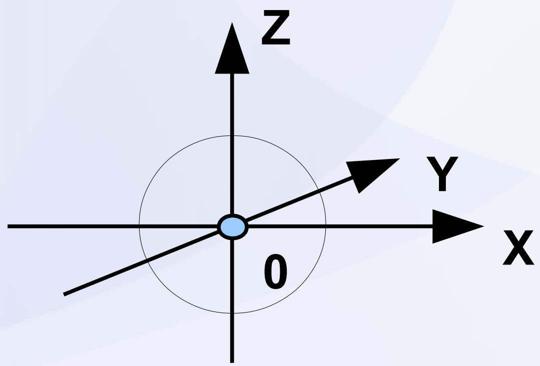


$$r=|q|=\sqrt{x^2+y^2+z^2};\quad dq=dx\,dy\,dz$$

$$\int \varphi_o\,dq=1;\quad \varphi_o(q)=\varphi_o(|q|)$$

$$w(q)=g^2\otimes\varphi_o=\int g^2(|q_1|)\varphi_o(q-q_1)\,dq_1$$

## π-meson

$$E_{ref}=(\psi,\hat{E}_{ref}\psi);$$

$$(f_1,f_2)=\int \tilde{f}_1 f_2\,dq$$

$$P=\frac{1}{c}\left(\frac{\partial\psi}{\partial t},W\frac{\partial\psi}{\partial t}\right);\quad W(q)=w_{max}-w(q)$$

$$\frac{\partial(\psi,\hat{E}_{ref}\psi)}{\partial t}=-\frac{1}{c}\left(\frac{\partial\psi}{\partial t},W\frac{\partial\psi}{\partial t}\right)$$

# 11. K-meson and η-meson

## K-meson

$$E_s = -\frac{1}{2}(\psi, \Delta\psi); \quad \Delta = \frac{\partial^2}{\partial x^2} + \frac{\partial^2}{\partial y^2} + \frac{\partial^2}{\partial z^2} \qquad E_t = \frac{1}{2c^2}\left(\frac{\partial\psi}{\partial t}, \frac{\partial\psi}{\partial t}\right);$$

$$\partial\left\{\frac{1}{c^2}\left(\frac{\partial\psi}{\partial t}, \frac{\partial\psi}{\partial t}\right) - (\psi, \Delta\psi)\right\}/\partial t = -\frac{2}{c}\left(\frac{\partial\psi}{\partial t}, W\frac{\partial\psi}{\partial t}\right) \longrightarrow \frac{1}{c^2}\frac{\partial^2\psi}{\partial t^2} - \Delta\psi + \frac{W}{c}\frac{\partial\psi}{\partial t} = 0$$

## η-meson

$$\frac{\partial u}{\partial t} + H u = 0; \quad H = \begin{pmatrix} cW & -c^2\Delta \\ -I & 0 \end{pmatrix}; \qquad u = U e^{\lambda t}; \qquad \{U_k\}, \{\tilde{U}_k\}; \ \{\lambda_k\}, \{\tilde{\lambda}_k\}.$$

$$\lambda U + H U = 0; \qquad A = \int g^2 dq$$

$$\lambda U + H_o U = 0; \quad H \rightarrow H_o; \quad w \rightarrow w_o; \quad w_o = B\varphi_o; \quad \lambda_n = \lambda_o$$

$$E_k = -m_k c^2 + i p_k c$$

$$\tilde{E}_k = -m_k c^2 - i p_k c$$

$$m_k = \frac{\hbar}{c^2}|\Re \lambda_k|; \quad p_k = \frac{\hbar}{c}\Im \lambda_k; \quad \lambda = \frac{E}{\hbar}, \quad \hbar = \frac{h}{2\pi}$$

$$u_k(q,t) = U_k e^{\lambda_k t} + \tilde{U}_k e^{\tilde{\lambda}_k t}, \ k = 1, 2, \ldots, n$$

# 12. The neutron

Under the influence of interaction with ether, its mode of correlation penetrates the η-meson impelling it to re-organize its separate modes of reflection into a collective, *organized mode of reflection*, represented by a *linear combination* of spatial wave functions,

$$F=\sum_{k=1}^{n} C_k U_k+\tilde{C}_k \tilde{U}_k;$$

where

$$C_k=\frac{(V_k, G)}{(V_k, U_k)}, \quad \tilde{C}_k=\frac{(\tilde{V}_k, G)}{(\tilde{V}_k, \tilde{U}_k)}; \qquad \lambda V+\bar{H} V=0; \quad (V_i, U_j)=0, \quad i\neq j$$

$\bar{H}$ - the matrix operator transposed to H; $G=\begin{pmatrix} g \\ g \end{pmatrix}$ - the two-component correlation function of ether. As a result, the η-meson turns into the neutron characterized by the correlation function spatially consistent with ether:

$$f(q,t)=\sum_{k=-n}^{n} C_k U_k \mathrm{e}^{\lambda_k t}; \quad a_{-k}=\tilde{a}_k$$

Thus the neutron is a linear system with continuously distributed parameters.

# 13. The H-atom

In the neutron, the form of its spatial wave functions $\{U_k\}$ contradicts the discrete character of its oscillation modes $\{e^{\lambda_k t}\}$. As a result, under interaction with ether, the continuously distributed parameters mass into lumped parameters thus transforming the neutron into the H-atom. The latter is characterized by the set of equations

$$\alpha_k \frac{d^2\varphi_k}{dt^2} + \beta_k \frac{d\varphi_k}{dt} + \gamma_k \varphi_k = 0\,;\; k = 1, 2, \ldots n$$

or by the vector equation

$$A\frac{d^2\boldsymbol{\Phi}}{dt^2} + B\frac{d\,\boldsymbol{\Phi}}{dt} + \Gamma\boldsymbol{\Phi} = 0\,; \quad \boldsymbol{\Phi} = \begin{pmatrix} \varphi_1 \\ \varphi_2 \\ \ldots \\ \varphi_n \end{pmatrix} \quad A = (a_{ik}) = \begin{pmatrix} \alpha_{11} & \alpha_{12} & \ldots & \alpha_{1n} \\ \alpha_{21} & \alpha_{22} & \ldots & \alpha_{2n} \\ \ldots\ldots & \ldots\ldots & \ldots & \ldots\ldots \\ \alpha_{n1} & \alpha_{n2} & \ldots & \alpha_{nn} \end{pmatrix}; \quad B = (\beta_{ik})\,; \quad \Gamma = (\gamma_{ik})$$

The structural function of the H-atom

$$\boldsymbol{u}(\boldsymbol{t}) = \sum_{k=-n}^{n} T_k \boldsymbol{U}_{\boldsymbol{k}} \mathrm{e}^{\lambda_k t}\,; \quad a_{-k} = \tilde{a}_k\,; \qquad \boldsymbol{u} = \begin{pmatrix} \frac{d\Phi}{dt} \\ \Phi \end{pmatrix}; \quad \boldsymbol{U}_{\boldsymbol{k}} = \begin{pmatrix} U_{k1} \\ U_{k2} \\ \ldots \\ U_{kn} \end{pmatrix},$$

Matrices A, B, Γ represent quarks, functions $\frac{d^2\boldsymbol{\Phi}}{dt^2}, \frac{d\,\boldsymbol{\Phi}}{dt}, \boldsymbol{\Phi}$ represent gluons.

# 14. Models and dynamics of the H- atom

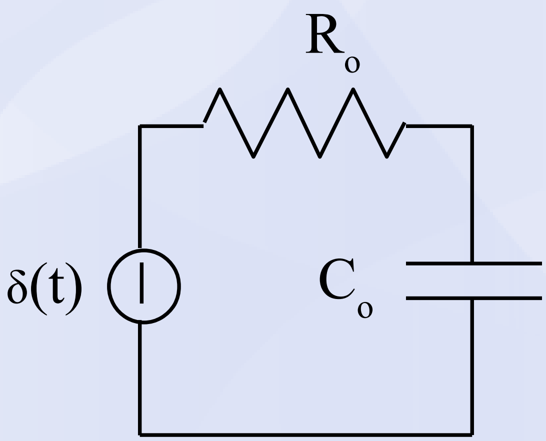


**The rough model of the H-atom**

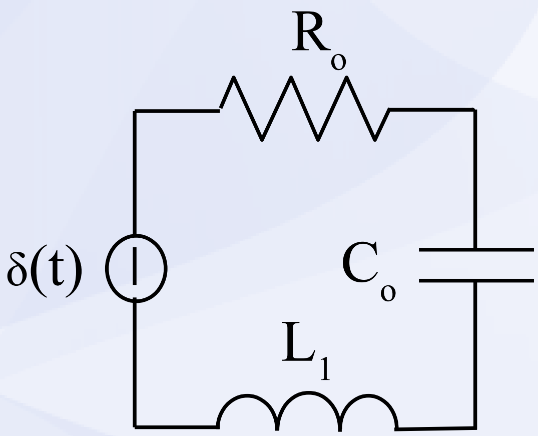


**The exact model of the H-atom**

Response: $q(t) \propto \exp(-\frac{t}{\tau_C})$; $\tau_C = R_o C_o$; $\quad q(t) \propto \exp(p_1 t) - \exp(p_2 t)$

Spectrum: $|Q(x)|^2 \propto \frac{1}{1+x^2}$; $x = \omega\tau_c$; $\quad |Q(\omega)|^2 \propto \frac{1}{(\omega^2+p_1^2)(\omega^2+p_2^2)}$

$${p^2}_1 \ll {p^2}_2$$

# 15. Models and dynamics of the neutron

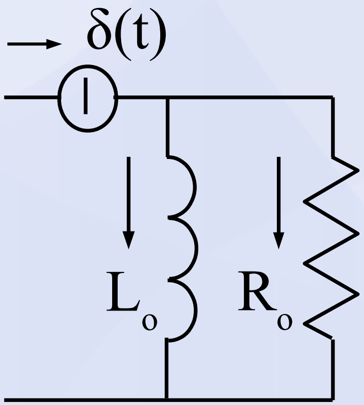


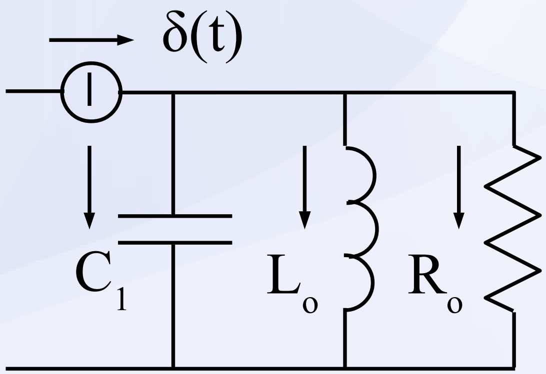


**The rough model of the neutron** **The exact model of the neutron**

Response: $i_R(t) \propto \exp(-\frac{t}{\tau_L}); \ \tau_L = \frac{L_o}{R_o}$ $i_R(t) \propto \exp(p_1 t) - \exp(p_2 t)$

General property of space: $\frac{L_o}{C_o} = \frac{L_1}{C_1} = R_o^2$

# 16. Models and dynamics of the D-atom

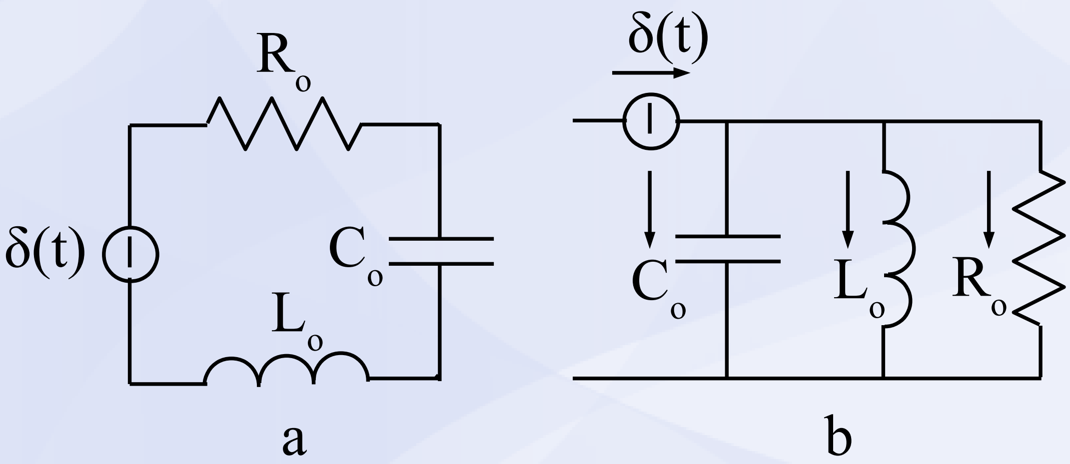


**The rough models of the D-atom:**
**(a) electric excitation, (b) magnetic excitation**

Response: $i(t) \propto e^{-\alpha t}\left(\cos\sqrt{3}\alpha t - \frac{1}{\sqrt{3}}\sin\sqrt{3}\alpha t\right);\quad \alpha = \frac{R_o}{2L_o};\ \ \omega_o^2 = \frac{1}{L_o C_o}$

The exponent factor $\alpha$ is half of that in the H-atom and the neutron, which means a higher structural efficiency of the D-atom than that of its components, and therefore a more efficient mode of energy conservation.

# 17. Model and dynamic of the He-atom

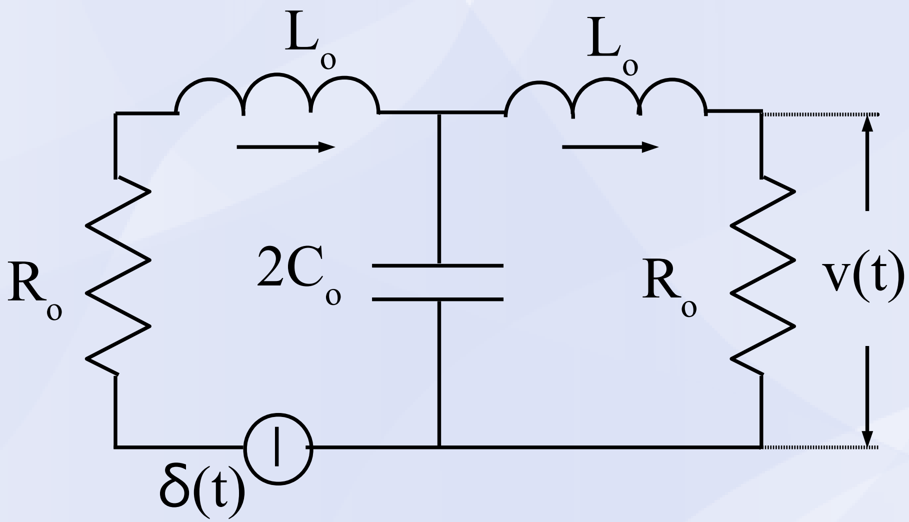


Response

$$v(t) \propto e^{-2\alpha t} + e^{-\alpha t}\left(\frac{1}{\sqrt{3}}\sin\sqrt{3}\,\alpha t - \cos\sqrt{3}\,\alpha t\right)$$

Spectrum:

$$|V(x)|^2 \propto \frac{1}{1+x^6}; \quad x = \frac{\omega}{\omega_o}$$

**The rough model of the He-atom**

Parameters of the models:

$$R_o \approx 376.7\,\Omega,$$

$$L_o = 4.17\times10^{-22}\,H, \quad C_o = 2.94\times10^{-27}\,F,$$
$$L_1 = 2.09\times10^{-23}\,H, \quad C_1 = 1.48\times10^{-28}\,F.$$

Fundamental frequency:

$$f_o = \frac{1}{2\pi\sqrt{L_o C_o}} = 1.44\times10^{23}\,Hz$$

Quantum energy:

$$E = hf_o \approx 9.54\times10^{-11}\,J \approx 5.95\times10^{8}\,eV.$$

# 18. Spectra of light atoms and ether

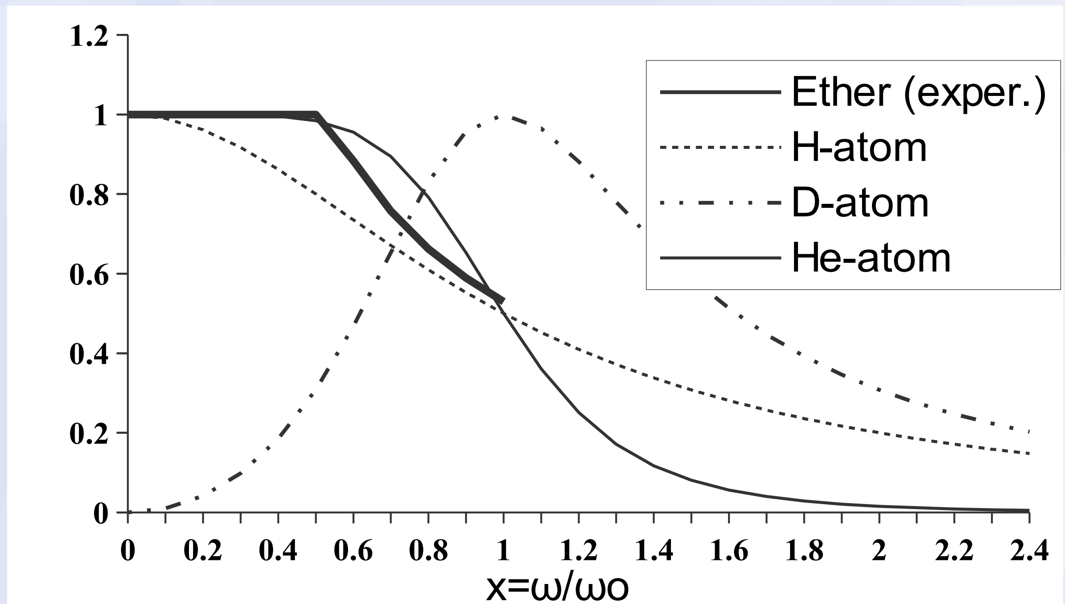


**Spectral functions of the atoms**

The comparison shows:

(1) the spectrum of the H-atom coincides with that of ether above energy $6\times10^{8}eV$ ;

(2) the He-atom and more complex ones form the cut-off region of ether, $10^{8.5}eV$.

# 19. Nuclear structure. Tetrahedral shell

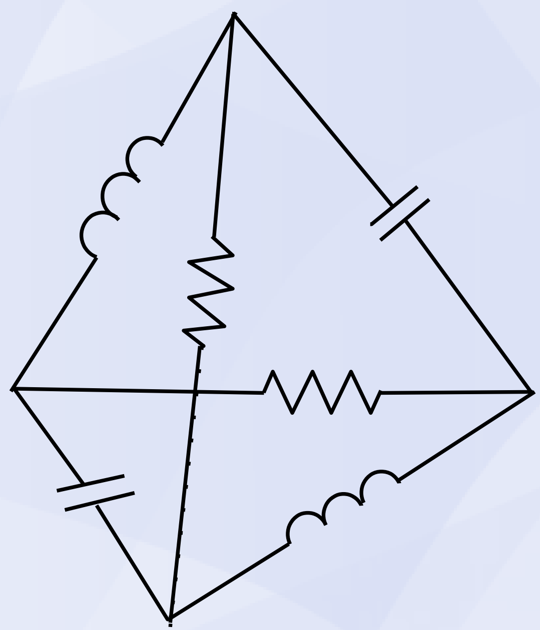

**The model of the tetrahedral shell**

Matrix of impedances

$$(Z_{4\times4})=\begin{pmatrix} Z & -R & -Z_C & -Z_L \\ -R & Z & -Z_L & -Z_C \\ -Z_C & -Z_L & Z & -R \\ -Z_L & -Z_C & -R & Z \end{pmatrix}$$

$$Z_L = pL,\quad Z_C = \frac{1}{pC},\quad Z = Z_L + Z_C + R$$

This shell is incompatible with the center and develops into the octahedral shell.

# 20. Nuclear structure. Octahedral shell

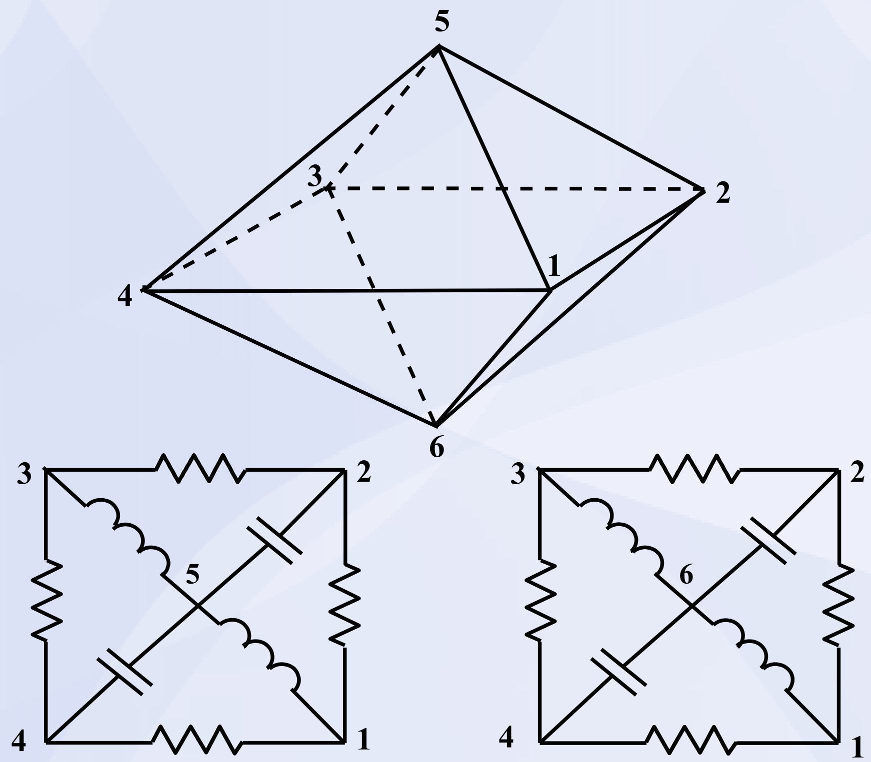


**The model of the octahedral shell**

The 8-shell suggests the existence of a sphere and develops into the 18-shell.

# 21. Nuclear structure. Icosahedral shell

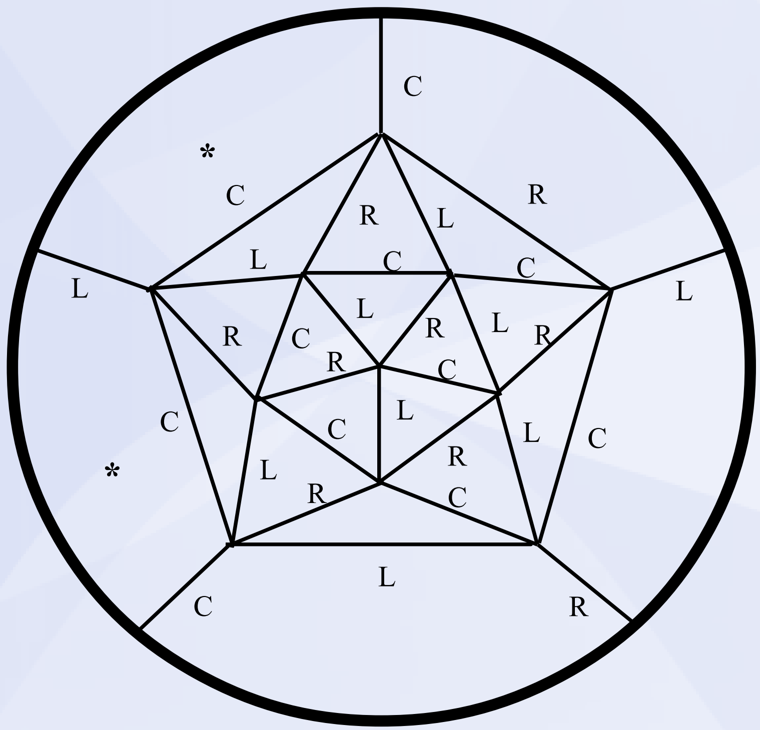


**The model of the icosahedral shell**

The 18-shell has 20 meshes but only 18 complete meshes represent D-atoms.

# 22. Complete system of shells

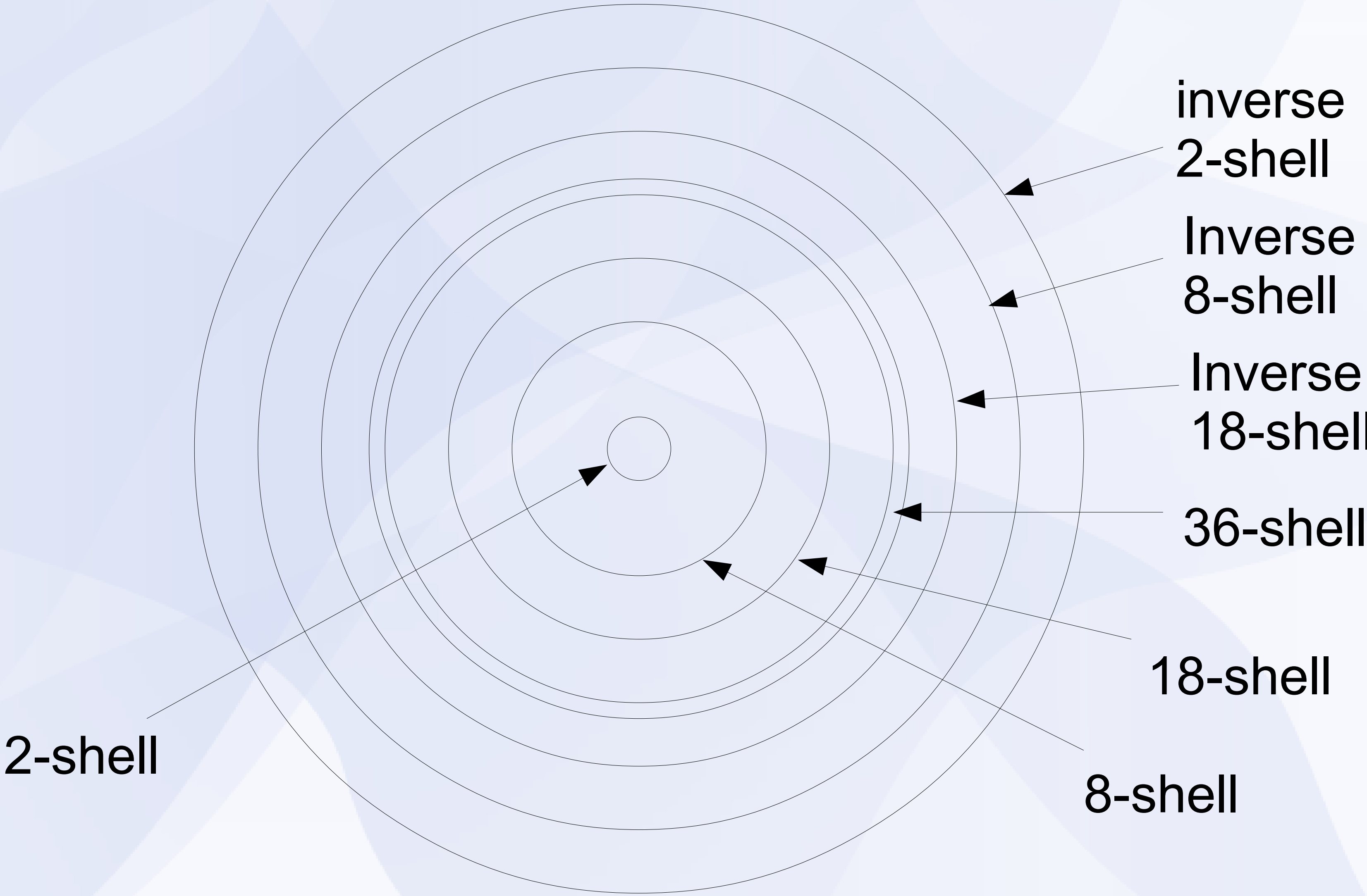

# 23. Nuclear structure of the *m*-atom

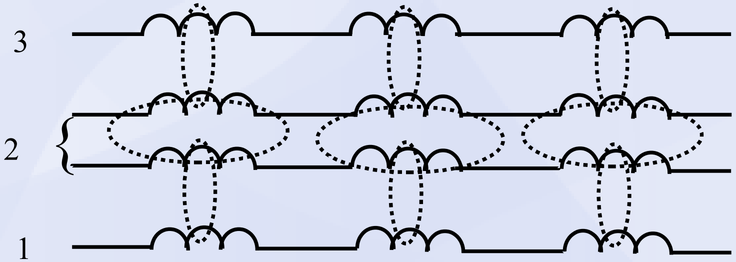


**The model of interaction of the 18-shells:**
**1- internal 18-shell; 2- central 36-shell;**
**3 – external 18-shell.**

Equation modeling the process of the *m*-atom:

$$\boldsymbol{L}\frac{d^2\boldsymbol{Q}}{dt^2}+\boldsymbol{R}\frac{d\boldsymbol{Q}}{dt}+\boldsymbol{D}\boldsymbol{Q}=0$$

$$\boldsymbol{L}=\left(L_{ik}\right),\quad \boldsymbol{R}=\left(R_{ik}\right),\quad \boldsymbol{D}=\left(D_{ik}\right)$$

$$D_{ik}=\frac{1}{C_{ik}},\qquad I_k=\frac{dQ_k}{dt},\qquad \boldsymbol{Q}=\begin{pmatrix}Q_1\\Q_2\\\dots\\Q_m\end{pmatrix}$$

The 4m-component vector function of response

$$\boldsymbol{f}_{\boldsymbol{m}}(t)=\sum_{k=-m}^{m}F_{mk}\boldsymbol{A}_{\boldsymbol{k}}\exp(\lambda_k t);\quad \sum_{k=-m}^{m}F_{mk}\boldsymbol{A}_{\boldsymbol{k}}=0;\qquad \boldsymbol{A}_{\boldsymbol{k}}=\begin{pmatrix}A_{k1}\\A_{k2}\\\dots\dots\\A_{km}\end{pmatrix}$$

In the U-atom, m=n=92, the response becomes a scalar function of parameter s=r=ct:

$$g_n(s)=\sum_{k=-n}^{n}S_k\exp(\chi_k s)\approx g(s)$$

presenting the most perfect approximation of the correlation function of ether.

# Reference-1

**Spectrum of cosmic electrons**
David Layzer. *Constructing the Universe.* 1984.



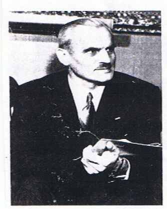

Arthur H. Compton (1892–1962).

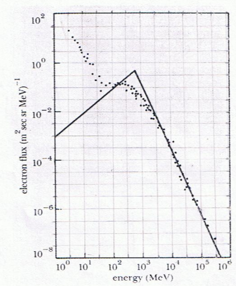


Observed spectrum of cosmic-ray electrons. The solid line represents the energy spectrum of "primary" electrons—electrons actually produced in the source, rather than by collisions between primary cosmic-ray protons and ambient nuclei.

Early in 1976 I suggested to Craig Hogan, then a senior at Harvard, that he look for a mechanism by which the early generation of massive stars that Hively and I had postulated to explain the microwave background might also produce the X- and gamma-ray background. After rejecting several candidate mechanisms, Hogan came up with one that looked promising. Supernovae (massive stars in the explosive stage of their evolution) are known to eject magnetized clouds of ionized gas that contain extremely energetic electrons. Arthur H. Compton had shown in the 1920s that when X-ray photons are scattered by electrons they give up some of their energy and momentum to the electrons. The inverse process can also occur: if the electrons are very energetic, they will lose energy to the photons. Hogan conjectured that the extremely energetic electrons that are a by-product of the supernova explosion would "collide" with ambient ultraviolet photons and promote them to X-ray photons.

The theory of such collisions is well-known, but to test his idea, Hogan and I needed to know how much energy a supernova puts into electrons and how that energy is distributed among them. This information could be extracted from experimental data on cosmic-ray electrons. These extremely energetic particles, detected by instruments mounted on rockets and satellites, are thought to be produced by supernovae in our Galaxy. Their energy spectrum has been accurately measured (see figure above). From the estimated rate of occurrence of supernovae in

# Reference-2

**Spectrum of cosmic rays.** Encyclopedia of Physics. 1990

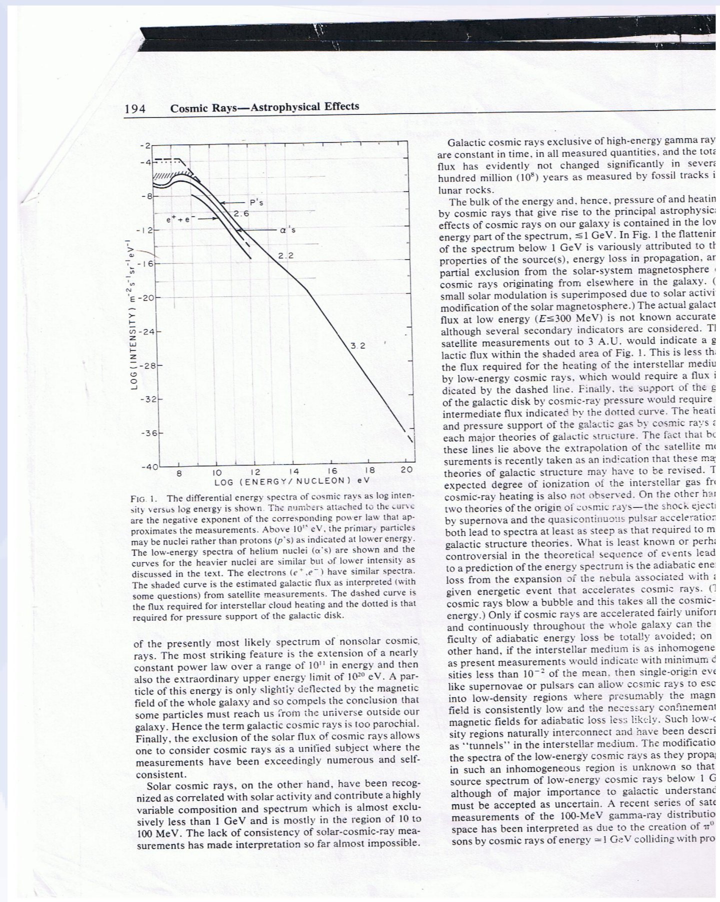





FIG. 1. The differential energy spectra of cosmic rays as log intensity versus log energy is shown. The numbers attached to the curve are the negative exponent of the corresponding power law that approximates the measurements. Above $10^{15}$ eV, the primary particles may be nuclei rather than protons ($p$'s) as indicated at lower energy. The low-energy spectra of helium nuclei ($\alpha$'s) are shown and the curves for the heavier nuclei are similar but of lower intensity as discussed in the text. The electrons ($e^+, e^-$) have similar spectra. The shaded curve is the estimated galactic flux as interpreted (with some questions) from satellite measurements. The dashed curve is the flux required for interstellar cloud heating and the dotted is that required for pressure support of the galactic disk.

of the presently most likely spectrum of nonsolar cosmic rays. The most striking feature is the extension of a nearly constant power law over a range of $10^{11}$ in energy and then also the extraordinary upper energy limit of $10^{20}$ eV. A particle of this energy is only slightly deflected by the magnetic field of the whole galaxy and so compels the conclusion that some particles must reach us from the universe outside our galaxy. Hence the term galactic cosmic rays is too parochial. Finally, the exclusion of the solar flux of cosmic rays allows one to consider cosmic rays as a unified subject where the measurements have been exceedingly numerous and self-consistent.

Solar cosmic rays, on the other hand, have been recognized as correlated with solar activity and contribute a highly variable composition and spectrum which is almost exclusively less than 1 GeV and is mostly in the region of 10 to 100 MeV. The lack of consistency of solar-cosmic-ray measurements has made interpretation so far almost impossible.

Galactic cosmic rays exclusive of high-energy gamma ray are constant in time, in all measured quantities, and the tota flux has evidently not changed significantly in severa hundred million ($10^8$) years as measured by fossil tracks i lunar rocks.

The bulk of the energy and, hence, pressure of and heatin by cosmic rays that give rise to the principal astrophysic effects of cosmic rays on our galaxy is contained in the lov energy part of the spectrum, $\lesssim$1 GeV. In Fig. 1 the flattenir of the spectrum below 1 GeV is variously attributed to th properties of the source(s), energy loss in propagation, ar partial exclusion from the solar-system magnetosphere cosmic rays originating from elsewhere in the galaxy. ( small solar modulation is superimposed due to solar activi modification of the solar magnetosphere.) The actual galact flux at low energy ($E \lesssim 300$ MeV) is not known accurate although several secondary indicators are considered. Tl satellite measurements out to 3 A.U. would indicate a g lactic flux within the shaded area of Fig. 1. This is less th the flux required for the heating of the interstellar mediu by low-energy cosmic rays, which would require a flux i dicated by the dashed line. Finally, the support of the g of the galactic disk by cosmic-ray pressure would require intermediate flux indicated by the dotted curve. The heati and pressure support of the galactic gas by cosmic rays each major theories of galactic structure. The fact that bo these lines lie above the extrapolation of the satellite me surements is recently taken as an indication that these ma theories of galactic structure may have to be revised. T expected degree of ionization of the interstellar gas fr cosmic-ray heating is also not observed. On the other ha two theories of the origin of cosmic rays—the shock ejecti by supernova and the quasicontinuous pulsar acceleratio both lead to spectra at least as steep as that required to m galactic structure theories. What is least known or perh controversial in the theoretical sequence of events lead to a prediction of the energy spectrum is the adiabatic ene loss from the expansion of the nebula associated with given energetic event that accelerates cosmic rays. (T cosmic rays blow a bubble and this takes all the cosmic- energy.) Only if cosmic rays are accelerated fairly unifor and continuously throughout the whole galaxy can the ficulty of adiabatic energy loss be totally avoided; on other hand, if the interstellar medium is as inhomogene as present measurements would indicate with minimum d sities less than $10^{-2}$ of the mean, then single-origin eve like supernovae or pulsars can allow cosmic rays to esc into low-density regions where presumably the magn field is consistently low and the necessary confinement magnetic fields for adiabatic loss less likely. Such low-c sity regions naturally interconnect and have been descri as "tunnels" in the interstellar medium. The modificatio the spectra of the low-energy cosmic rays as they propa in such an inhomogeneous region is unknown so that source spectrum of low-energy cosmic rays below 1 G although of major importance to galactic understand must be accepted as uncertain. A recent series of sate measurements of the 100-MeV gamma-ray distributio space has been interpreted as due to the creation of $\pi^0$ sons by cosmic rays of energy $\simeq$1 GeV colliding with pro

# Cognizance of Nature